The College of Engineering
University of Wisconsin-Madison

Wisconsin Electric Machines and Power Electronics Consortium

RESEARCH REPORT
90-17

Calculations of Electromagnetic Fields Including End Effect Using Fourier Transform Method

Azza A. Fahim, T.A. Lipo,
Dept. of Elec. and Comp. Eng.
University of Wisconsin-Madison
1415 Johnson Drive
Madison, WI 53706-1691

WEMPEC

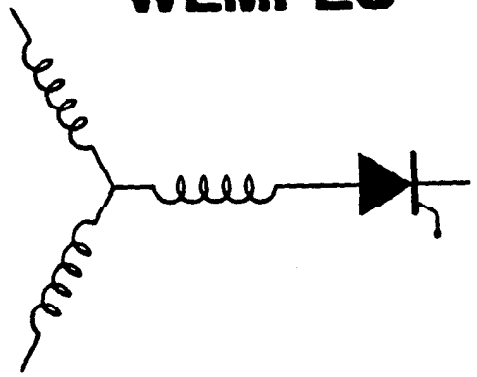

Department of Electrical and Computer Engineering
1415 Johnson Drive
Madison, Wisconsin 53706

Calculations of Electromagnetic Fields Including End Effect Using Fourier Transform Method

Azza A. Fahim T. A. Lipo

Dept. of Electrical & Computer Eng.
University of Wisconsin - Madison
Madison, WI 53706, U.S.A.

Abstract A Fourier transform technique has been used to provide an analytical solution for the 3-D magnetic field associated with air core windings. The method is applied to study an electromagnetic design aspect of a superconducting machine. Special attention is given to the screen induced current with the effect of the end winding included.

1. Introduction

There are many areas in electrical machine design where three dimensional electromagnetic field analysis is required. Examples are in linear types of ac machines and in protective shields of electrical apparatus. At present must interest is directed, in particular, to the field analysis of superconducting machines. The nature of the air core winding and the existence of both magnetic and conducting screens as suggested by some designs [1-2] necessitate a three dimensional (3-D) field analysis. At the same time, the limitations imposed by the electromagnetic specifications of the newly developed high temperature superconducting (HTSC) winding requires an accurate prediction of the field at the machine end region where high field values are expected [3].

Early work on air core machines was based on 2-D solutions [4], where the end regions are ignored. Unfortunately the available 3-D numerical solution based on the Finite Element Method (FEM) can be very time consuming in the early stage of the design since the solution is specific to a particular configuration. On the other hand, the accuracy of published three dimensional analytical solutions based on image method [5] and the correction factor for 2-D solution [6] are limited since they rely on numerous approximations.

In this paper, we present a novel method for calculating 3-D magnetic fields using the Fourier transform technique. A significant advantage of this approach is its flexibility in accommodating arbitrary geometries of the winding and the boundaries. In addition, advantage is obtained in the programming simplicity.

The analysis begins by considering the air-core coils as two parts, straight conductors and end turns, and determining the field produced by each part separately. By employing the Fourier transform technique, the field produced by finite-length excitation is easily found. The 3-D field solution is then obtained by superposition of the solutions of the main winding and the end turns.

This paper investigates in simple terms the relationship between the field distribution and the air core winding geometry. The dimensions of most importance are the radii and lengths of both the winding main coil and the overhang windings (end turns). Because of the central importance of the shielding effect of the screen in the design of SC machines, special attention is paid to the induced current produced in an infinitely long conducting screen. In a future paper we will report an analysis of the finite axial length of the screen.

2. Electromagnetic Field Analysis

2.1 Winding Configuration

A general model of the SC machine capable of representing the problem consists of a 2-pole, 3-phase air core armature winding enclosing a rotor conductive cylinder (SC shield). In this model, all the boundaries are cylindrical surfaces and the axial rotor cylinder extends beyond both ends of the armature winding. The armature winding is arranged in coil groups, each coil has the basic saddle shape shown in Fig. 1. The straight parts of the coils forms the main winding where the current is axially oriented. The return paths of the coils are arcs of filaments laying on the periphery of a circle and forming the end windings where the return current is circumferentially directed.

The field distribution caused by the above

winding configuration has a three dimensional (3D) nature. However, since the media in this problem are linear (no iron is involved), the field produced by the main winging and the end windings can be solved separately. Each winding is a finite -length current source that creates a 2-D field. The overall 3-D solution is then obtained by superposition. To ensure consistency of the 3-D solution, the current sources in the two problems and the overall field solutions must satisfy the continuity condition.

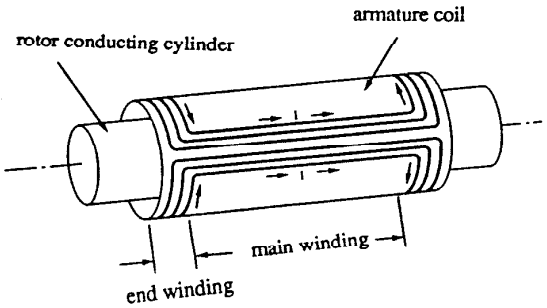

Fig.1 Basic coil configuration

2.2 Electromagnetic Field Model

A cross section of the model in the (r-z) plane is shown in Fig.2, where l_s is the average length of the main winding and w_R is the end winding (ring) width. R_s and R_a are the mean radii of the stator and the rotor-shield cylinder, respectively.

The regions where the field distribution is of the most interest are:

Region (1)	(SC region)	$0 \le r \le R_a$
Region (2)	(air core)	$R_a \le r \le R_s$
Region (3)	(outermost air)	$R_s \le r \le \infty$

In this model, the conductive cylinder is assumed to be infinitely long and the environmental magnetic shield is not considered.

The general partial differential equation PDE describing the field in the different regions in terms of the magnetic vector potential A using cylindrical coordinates is :

$$\frac{\partial^2 \bar{A}}{\partial r^2} + \frac{1}{r}\frac{\partial \bar{A}}{\partial r} + \frac{1}{r^2}\frac{\partial^2 \bar{A}}{\partial \theta^2} + \frac{\partial^2 \bar{A}}{\partial z^2} = -\mu_0(\bar{J}_s + \bar{J}_e) \quad (1)$$

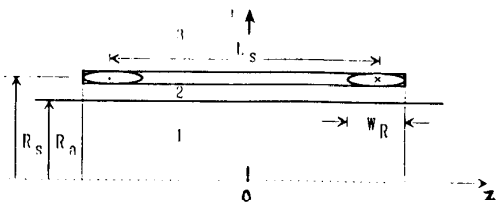

Fig.2 Model cross section

where $\bar{J}_s$ is the source current density vector and

$$\bar{J}_e = -j\omega\mu_0\sigma\,\bar{A} \quad (2)$$

is the shield induced current density, wherein ω is the angular frequency of the excitation current and σ is the volumetric conductivity of the shield.

For the winding configuration (Fig. 1), the source current density vector has an axial (main winding) and a circumferential (end winding) component, J_{sz} and $J_{s\theta}$, respectively, so that

$$\bar{J}_s = J_{sz}\,\bar{a}_z + J_{s\theta}\,\bar{a}_\theta \quad (3)$$

Consequently, the magnetic vector potential $\bar{A}$ and the induced current density vector $\bar{J}_e$ also have axial and circumferential components.

Decomposing the components of the field vector, Eq. (1), the solution can be obtained by solving two separate PDEs corresponding to the two current sources J_{sz} and $J_{s\theta}$. The two current densities have distributions extending over a finite axial length and their values are related since the total current must be continuous.

3. Fourier Transform Approach

For a prescribed distribution of the current source in the θ direction, each component of Eq. (1) reduces to a 2-D problem. An analytical solution of such an equation is available only when $\bar{J}_s$ is independent of z, i.e. the excitation is constant and extends indefinitely, which is obviously not the case. To handle this problem, the Fourier transform (FT) method is used. The essential concept of this approach is to replace the localized

current by a sum or integral of harmonically excited (continuous) current sheets. The solution for each harmonic source can be obtained directly by solving a scalar PDE.

3.1 Current Source:

The expansion of an arbitrary function $J_s(z)$ as an integral of harmonic functions is expressed by use of FT equations [7].

$$J_s(z) = \frac{1}{2\pi} \int_{-\infty}^{\infty} J_s(\beta)\, e^{-j\beta z}\, d\beta \qquad (4)$$

and

$$J_s(\beta) = \int_{-\infty}^{\infty} J_s(z)\, e^{j\beta z}\, dz \qquad (5)$$

where $J_s(\beta)$ is called the FT of $J_s(z)$ and β is the spatial frequency ($\beta=2\pi/\lambda$) and λ is the harmonic wave length.

The components $J_s(\beta)e^{-j\beta z}$ in the expression, Eq. (4), are harmonically excited current sources of constant amplitudes $J_s(\beta)$ and different frequencies β. The field solution $A(\beta)$, which is generated by each of these components is obtained, as in conventional solutions of infinitely long models, by solving the boundary value problem.

3.2. Field Solution Due to Finite-length Excitation:

The next step is to calculate the required solution A(z) for the field due to a finite excitation source. According to Eq. (4), the inverse Fourier Transform is obtained as:

$$A(z) = \frac{1}{2\pi} \int_{-\infty}^{\infty} A(\beta)\, e^{-j\beta z}\, d\beta \qquad (6)$$

The actual implementation of Eq. (5) and the superposition in Eq. (4) is performed by use of the discrete approximation (the discrete Fourier transform) and the fast Fourier transform (FFT) algorithm, as will be explained later.

4. Application of the Method

4.1. Field Due to Main Winding Excitation

For a sinusoidally distributed armature coils, the main winding is represented by a current sheet of finite length L_s localized at radius R_s, which can be expressed as the rectangular function

$$\bar{J}_s(r,\theta,z) = J_m \cos p\theta\, \bar{a}_z, \quad -L_s/2 \le z \le L_s/2$$
$$= 0, \quad \text{elsewhere} \qquad (7)$$

where 2p is the machine number of poles, and

$$J_m = \frac{3\,NI}{(2\pi/2p)\, r_{sa}\, \Delta r_s} \qquad (8)$$

r_{sa} = mean radius of the main winding
Δr_s = thickness of main winding
N = Number of turns/phase
I = phase current

The Fourier Transform of Eq. (7), is

$$Js(\beta) = J_m \frac{\sin\beta L_s/2}{\beta/2} \cos p\theta \qquad (9)$$

Solution for a Harmonically Excited Source:

For a harmonically excited current source where $J_s(\beta)e^{-j\beta z}$, the field PDE. reduces to

$$\frac{\partial^2 A}{\partial r^2} + \frac{1}{r}\frac{\partial A}{\partial r} - \{\frac{p^2}{r^2} + \beta^2 + j\omega\mu_0\sigma\}A = -\mu_o J_m \frac{\sin\beta L_s/2}{\beta/2} \qquad (10)$$

The analytical solution of Eq. (10) is in terms of the modified Bessel functions $I_1(\beta r)$ and $K_1(\beta r)$. For the model described in section (2.2), and for A=0 at r=0 and r= ∞ the solution $A(\beta,r)$ in the model for the different regions are:

$0 \le r \le R_a$
$$A_1(\beta,r) = C_1 I_1(\beta r) \qquad (11)$$

$R_a \le r \le R_s$
$$A_2(\beta,r) = C_2\, I_1(\beta r) + D_2\, K_1(\beta r) \qquad (12)$$

$R_s \le r \le \infty$
$$A_3(\beta,r) = D_3\, K_1(\beta r) \qquad (13)$$

where C_1, C_2, D_2 and D_3 are the solution constants determined from defined from the boundary conditions between the regions.

Boundary Conditions

For the axially oriented excitation the boundary conditions in terms of the magnetic vector potential $A(\beta,r)$ are:

at $r = R_a$,
$$A_2(\beta,r) = A_1(\beta,r) \qquad (14)$$
$$\frac{\partial}{\partial r} A_2(\beta,r) - \frac{\partial}{\partial r} A_1(\beta,r) = j\omega\, \mu_o\sigma\, \Delta r_a\, A_1(\beta,r) \qquad (15)$$

at $r = R_s$,
$$A_3(\beta,r) = A_2(\beta,r) \qquad (16)$$
$$\frac{\partial}{\partial r} A3(\beta,r) - \frac{\partial}{\partial r} A2(\beta,r) = -\mu_o J_S \Delta r_S \qquad (17)$$

where Δr_a is the thickness of the shield conductive cylinder.

Final values for the field solution A(z,r) in the model different regions (r=0, r=∞) is then obtained by performing inverse Fourier Transform of Eqs. (11,12,13) .

4.2. Field due to End Winding Excitation

Current Source

Since the end turns are the physical continuation of the main winding, the excitation current due to each end winding is

$$\bar{J}_{s\theta}(R_s,\theta,z) = \pm J_m(z)\sin p\theta\,\bar{a}_\theta, -w_R/2 \le z \le w_R/2$$
$$= 0 \quad , \text{elsewhere} \qquad (18)$$

where the ± refers to the orientation of the current in the right and the left ends, respectively and

$$J_m = \frac{3\,NI/2p}{w_R\,\Delta r_s} \qquad (19)$$

The solution for the harmonically excited source is obtained by solving the boundary value problem. The boundary conditions in this case where J_s is circumferentially directed are:

at $r = R_a$,

$$A_2(\beta,r) = A_1(\beta,r) \qquad (20)$$

$$\frac{\partial}{\partial r}A_2(\beta,r) - \frac{\partial}{\partial r}A_1(\beta,r) = -j\omega\mu_o\sigma\Delta r_a A_1(\beta,r) \qquad (21)$$

at $r = R_s$,

$$A_3(\beta,r) = A_2(\beta,r) \qquad (22)$$

$$\frac{\partial}{\partial r}A_3(\beta,r) - \frac{\partial}{\partial r}A_2(\beta,r) = \mu_o J_s \Delta r_s \qquad (23)$$

Expressions for solution constants and the final distribution of A(z) is obtained similar to the main winding case.

4.3. Three Dimensional Field Solution:

In sections 4.1 and 4.2 the distribution for m.v.p. components, A_z and A_θ, in the model different regions (r=0, r=∞) are obtained as :

$$A_z(r,\theta,z) = A_z(r,z)\cos p\theta \qquad (24)$$

$$A_\theta(r,\theta,z) = A_\theta(r,z)\sin p\theta \qquad (25)$$

Applying the principle of superposition, the 3-D magnetic flux density components B_r, B_θ and B_z are obtained as:

$$B_r = B_{r|(main)} + B_{r|(end)} \qquad (26)$$

$$B_\theta = B_{\theta|(main)} \qquad (27)$$

$$B_z = B_{z|(end)} \qquad (28)$$

where (main) and (end) refers to the main winding and the end windings, respectively and the field flux density components in terms of the magnetic vector potential are:

$$B_{r|(main)} = \frac{1}{r}\frac{\partial A_z}{\partial \theta} \qquad (29)$$

$$B_{r|(end)} = \frac{\partial A_\theta}{\partial r} + \frac{A_\theta}{r} \qquad (30)$$

$$B_{\theta|(main)} = -\frac{\partial A_z}{\partial r} \qquad (31)$$

$$B_{z|(end)} = \frac{\partial A_\theta}{\partial \theta} \qquad (32)$$

4.4 Shield Induced Current.

The shield induced current due to the 3-D fields is obtained by computing the two components of the induced current density vector

$$J_e = J_{ez}\bar{a}_z + J_{e\theta}\bar{a}_\theta \qquad (33)$$

where

$$J_{ez}(R_a,\theta,z) = -j\omega\mu_o\sigma\, A_z(R_a,z)\cos p\theta \qquad (34)$$

$$J_{e\theta}(R_a,\theta,z) = -j\omega\,\mu_o\,\sigma\, A_\theta(R_a,z)\sin p\theta \qquad (35)$$

5. Case Study

Implementation of the analysis in this paper is straightforward except for the computation related to the Fourier Transform. Here we rely on the discrete approximation of the FT. For example, the discrete form of Eq. (6) is

$$A(n\,\Delta z) = \frac{\Delta\beta}{2\pi}\sum_{k=0}^{N-1} A(k\Delta\beta)\; e^{-jnk\Delta\beta\Delta z} \qquad (36)$$

where

Δz =unit interval of z

$\Delta\beta$ = unit interval of β

and $\Delta\beta$ and Δz are related by:

$$\Delta\beta\,\Delta z = \frac{2\pi}{N}$$

Choices of the parameters $\Delta\beta$ and Δz must carefully made to ensure accuracy of the results.

For a model machine of the dimensions given in Table I, the field distribution at the conductive screen surface $r = R_a$ and for $\theta = \pi/4$ (where $\theta = 0$ is the magnetic axis of the air core coils) have been calculated. The results for the magnetic flux density components due to the main winding $B_{rl(main)}$ and $B_{\theta l(main)}$ are shown in Fig. 3.

For the end windings, the current source function and the produced flux density components $B_r|_{(end)}$ and $B_z|_{(end)}$ are shown in Fig. 4. In all figures, the shield conductive cylinder is assumed to have infinite length. The effect of the excitation finite length (L_s and w_R) is quite remarkable on the resultant axial distribution of the field. Also from the amplitudes of the magnetic flux density components, the radial component $B_r|_{(end)}$ exhibits a relatively high value which confirm the expected high value of the field flux density at the machine end due to the end winding.

Calculated results for the induced current density components J_{cz} and $J_{c\theta}$ at the line of intersection between the conductive shield surface and an (r,z) plane located at $\theta = \pi/4$ is shown in Fig. 5. One of the useful points of information provided by this approach is to construct a contour plot for the shield induced current. A plot for the induced current density pattern plot can be obtained by calculating the amplitude and the space angle of the current density vector at different (θ,z) points over the conductive surface.

6. Conclusions

A newly developed analytical solution for the 3-D electromagnetic field produced by an air core winding is provided. The actual configuration of the winding is considered by taking into account the effect of the end windings. The analysis is based on employing Fourier transform technique to compute the field produced by a finite-length excitation. The analysis is applied to study the fields in superconducting machines which has an air core armature winding and a rotor conductive shield. The solution provides a distribution for the 3-D field components and the shield induced current.

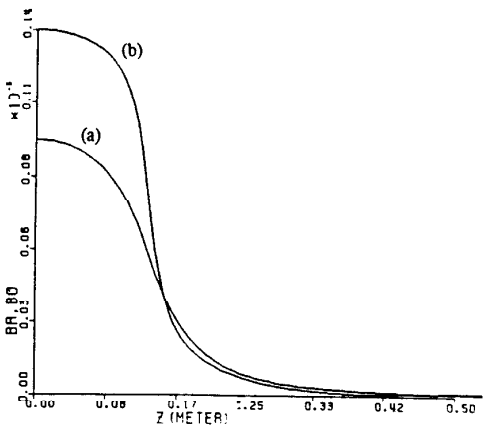

Fig. 3 Field produced by main winding
(a) $B_{rl(main)}$ (b) $B_{\theta l(main)}$

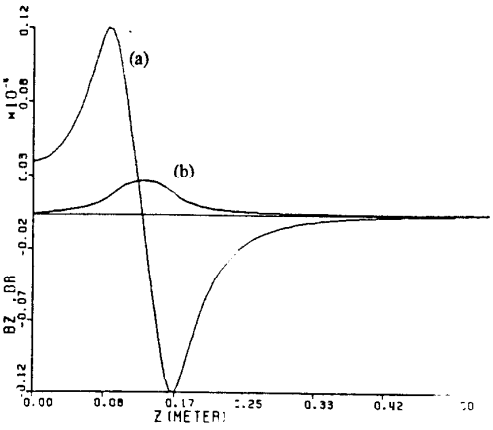

Fig.4 Field produced by endwinding
(a) $B_{rl(end)}$ (b) $B_{zl(end)}$

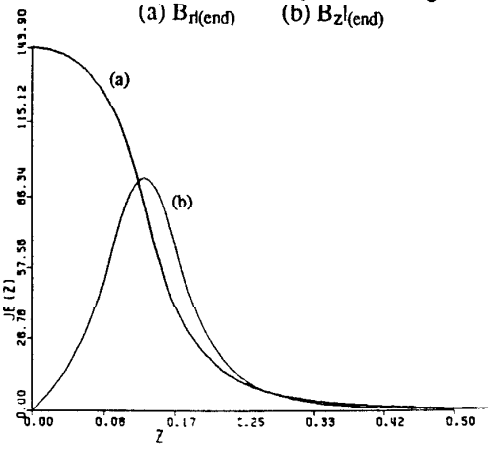

Fig. 5 Shield induced current
(a) J_{ez} (b) $J_{e\theta}$

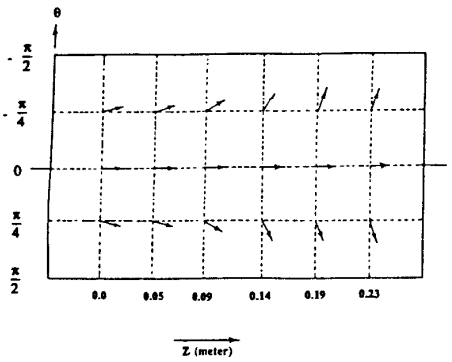

Fig.6 Shield induced current battern.

7. Acknowledgments

The authors gratefully acknowledge support of this work by the Electric Power Research Institute, Palo Alto CA under contract RP 3149-2.

References

[1] H.E. Jordan,"Feasibility Study of Electric Motors Constructed with High Temperature Superconducting Materials," Electric Machines and Power Systems, Vol. 16, No.1,1989, pp. 15-23.

[2] J.S. Edmonds, H.E. Jordan, J.D. Edick, R.F. Shiferl,"Application of High Temperature Superconducting Materials to Electric Motors," International Conference on Electrical Machines (ICEM), Cambridge MA, August 1990.

[3] S.E. Dorris, J.T. Dusek, M.T. Lanagan, J.J.Piccol, R.Russel and R.B. Poeppel, "$YBa_2CU_3O_x$ Superconductor Coil: Processing and Properties," International Conference on Electrical Machines (ICEM), Cambridge MA, August 1990.

[4] A. Hughes, T.J.E. Miller,"Analysis of Field and Inductances in Air-cored and Iron-cored Synchronous Machines," Proceedings of the IEE, Vol. 124, No 2, February 1977, pp. 121-126.

[5] Q. Li, and F. Wang,"Application of the Image Method to Calculate 3-D Magnetic Field and Parameters of SC Alternators," IEEE Trans. on Magnetics, Vol. 25, No. 2, March 1989, pp. 1850-1853.

[6] Y.H.A. Rahim, D.L. Prior, and C.V. Jones, "Air-Cored Alternators: A Numerical-Analytical Transient-Field Model," IEEE Trans. on Power Appraraus and Systems, Vol. 103, No. 7, July 1984, pp. 1773-1780.

[7] N. Ahmed and T. Natarajan, "Discrete-Time Signals and Systems", (book), Reston, Virginia 1983.

Table I

Total Amp.Turns	$3NI$	= 1.0	
Number of poles	$2p$	= 2	
Frequency	f	= 2	Hz
Conductivity	σ	= 132×10^6	mho/m
Main winding radius	R_s	= 0.08334	m
Cylinder radius	R_a	= 0.063505	m
Main winding length	L_a	= 0.26	m
End ring width	w_R	= 0.06675	m